Pergamon

Planet. Space Sci., Vol. 44, No. 8, pp. 833–841, 1996

0032–0633/96 $15.00+0.00

PII: S0032–0633(96)00011–6

Formation and evolution of the westernmost corona of Aphrodite Terra, Venus

V. Ansan[1] and Ph. Blondel[2]

[1]Laboratoire de Géologie Dynamique de la Terre et des Planètes, Bât. 509, Université Paris–Sud, 91405 Orsay cedex, France
[2]Institute of Oceanographic Sciences, Deacon Laboratory, Brook Road, Wormley, Godalming GU8 5UB, U.K.

Received 29 July 1995; accepted 13 December 1995

Abstract. Previous knowledge of Venus equatorial highlands has been greatly extended by Magellan SAR imagery. Spanning over more than 15,000 km, with a mean elevation of 3 km, Aphrodite Terra is a key region for the comprehension of Venusian geology and tectonics. Surface geology is investigated with the high-resolution Magellan radar imagery. This study focuses on the westernmost part of Aphrodite Terra, an area 2000 km in diameter centred on Verdandi Corona. Structural interpretation is based on conventional manual cartography and image processing. The conjunction of these two methods enables a model of formation to be proposed in four stages: (1) intense fracturation of the substratum under extensive stress, creating a pattern of small horsts and grabens, (2) filling of grabens by a volcanic material, (3) formation of Verdandi Corona, a circular feature 180 km wide, with concentric and radial fractures corresponding to the remains of a subsiding volcano, (4) N105° faults overcutting the caldera and radial normal faults developing at its periphery. Along with the topographic information available, these stages suggest that this corona results from the rising, cooling and flattening of a diapir intruded in the Venusian pre-existing fractured crust.

Introduction

Due to its thick and cloudy atmosphere, the surface of Venus can be only observed with radar. Since its injection into orbit in 1990, the Magellan probe has acquired many data including altimetry, gravity and radar images, for more than 90% of the surface of Venus (Saunders and Pettengill, 1991; Saunders *et al.*, 1991, 1992). The Magellan SAR (Synthetic Aperture Radar) has imaged 97% of the planetary surface with a high resolution varying from 120 m at the equator to 300 m at the pole. These images show that the surface is mainly affected by volcanic and tectonic processes (Saunders and Pettengill, 1991; Solomon and Head, 1991; Saunders *et al.*, 1991, 1992). On an altimetric map, a prominent feature is the equatorial highland of Aphrodite Terra (Fig. 1). It extends over 15,000 km along the equator, from approximately 45°E to 210°E, with a mean elevation of 3 km, and covers approximately 10% of the planet's surface (Phillips and Malin, 1983; Solomon *et al.*, 1992). Its topography is characterized by a series of circular features 2000–3500 km in diameter. The westernmost of these features corresponds to the western boundary of Ovda Regio, a plateau-shaped highland characterized by a rugged, radar-bright surface. This area is characterized topographically by a 2 km high, eastern half-ring bounding a plateau gently tilted to the west. At its centre, a 180 km wide circular depression, named Verdandi Corona, is observed (5.5°S–65°E). Our geologic and structural study focuses on this region of Aphrodite Terra, and is based on radar-mosaic F-MIDRP.05S065 (Fig. 2). This full-resolution image covers an area of approximately 250,000 km^2, with a pixel size of 75 m, allowing the resolution of hectometre-scale details. Classic manual methods of image interpretation are used with some caution, inherent to the interpretation of radar images (Ford *et al.*, 1989, 1993), in order to define the type, the style and the relative chronology of the Venusian crustal deformations. Its results are supplemented with image processing techniques (Blondel *et al.*, 1992), which provide maps of specific linear features and quantify their geometric parameters (length, direction and sinuosity). Much is gained from the conjunction of the two methods, as exposed in the subsequent tectonic interpretation. This

Correspondence to: V. Ansan

local geologic and structural study leads to the proposition of a model of formation for the region around Verdandi Corona, discussed and compared with models.

Methodology

Interpretation of radar imagery is not straightforward, compared to the interpretation of imagery in optical wavelengths (Ford *et al.*, 1989, 1993). Radar backscatter is related to the interaction of the micro-wave with the surface, which itself depends on radar characteristics (wavelength and polarization), the illumination geometry, and the surface characteristics (topography, micro-scale roughness, bulk dielectric properties); e.g. Ford *et al.* (1989, 1993). The Magellan SAR transmitted on a 12.6 cm wavelength, with a horizontal polarization (HH mode). The image considered in this study was acquired with a radar beam oriented to the east, and with a 44° incidence angle. Several models exist to describe the interaction of the radar with the surface, constrained by numerous experimental and theoretical studies on the planetary surface (Hagfors, 1964; Schaber *et al.*, 1976; Ulaby *et al.*, 1982). Combined with previous knowledge from Venus geology (e.g. Saunders *et al.*, 1992), they show that radar backscatter is mainly affected by the topographic slope with respect to the radar beam, and that topographic changes do not create noticeable geometric distortions (layover or foreshortening) (Ford *et al.*, 1989, 1993).

Bearing this in mind, conventional manual interpretation was performed on the large-scale photograph provided by NASA-JPL (F-MIDRP 05S065, browse image, supplemented by high-resolution images for detailed analysis). The individual geologic features (impact craters, volcanoes, faults, folds, etc.) were identified and mapped. Based on their respective distribution and orientation, these features are used to determine the local tectonics and the types and styles of deformation (compressive/extensive). Superposition and cross-cutting relationships induce the establishing of a relative chronology for the morpho-structural units. Because of the size and resolution of the dataset, this method may be excessively long (from a few hours to a few days). Loss of information occurs in complex areas, where features are numerous and intricate, and where manual interpretation tends to average the information, favouring the most remarkable structures.

Numerical processing can alleviate this problem and help the interpreter in complex regions. The technique called "Structure-Tracking" has been developed specifically for radar images of Venus (Blondel *et al.*, 1990, 1992). It has been validated on Venera 15–16 and Magellan data (Blondel *et al.*, 1992; Blondel, 1992), as well as on sonar images (Blondel *et al.*, 1993) and SPOT data (Luxey *et al.*, 1995). The "Structure-Tracking" technique detects linear features by their luminosity gradients, and tracks them with a searching pattern designed for geological features. Each structure detected is precisely located in the numerical image, and its parameters are computed: length (according to the projection), mean direction, histogram of directions, sinuosity. This technique gives the conventional interpretation, especially in complex regions, and supports it with quantitative information.

Interpretation of radar mosaic F-MIDRP.05S065

The Magellan mosaic F-MIDRP.05S065 (browse image) (Fig. 2) exhibits a pattern of radar-bright blocks on a radar-dark background, and a large circular feature, approximately 180 km in diameter, centred at latitude 5°S and longitude 65°E. The irregular radar-bright blocks rise a few thousands metres above the background (Leberl *et al.*, 1992), and are more or less equidimensional. Their surface shows a network of rectilinear troughs. The blocks are spaced by short, linear, radar-dark troughs. Their morphology is marked by linear, bright features corresponding to topographic scarps facing the radar beam on their western side, and dark, narrow features corresponding to topographic scarps opposite to the radar beam on their eastern side. The large circular feature, named Verdandi Corona, is bounded by a network of discontinuous, concentric, radar-bright linear features (Stofan *et al.*, 1992). A network of short, radial, radar-bright features is observed, essentially in the northern part of Verdandi Corona. Topographically, this feature corresponds to a circular depression with a 1200 m high rim. The inner part is characterized by a local plateau standing at 200 m above the background, and two depressions (Fig. 3). Furthermore, Verdandi Corona is crosscut by a set of approximately E–W trending, narrow, long, rectilinear features topographically marked by a 400 m high, WSW–ENE, linear depression, on the western side of Verdandi Corona (Fig. 3).

Drawn manually, the structural map is presented in Fig. 4A. The rectilinear topographic scarps bounding the radar-bright blocks are interpreted as fracture zones or normal-fault scarps. Consequently, the bright, raised blocks correspond to horsts, whereas the dark troughs correspond to grabens. They are filled with radar-dark material, interpreted as lava flows on the basis of their radar backscatter characteristics (Ford *et al.*, 1989). Because of their geometry and volcanic association, these troughs may have resulted from dike emplacement at depth combined with crustal fracturing at the surface (McKenzie *et al.*, 1992). However, in some place, radar-dark material interpreted as lava flows partially cover the pattern of bright blocks (Fig. 2, around the circular feature, Verdandi Corona). On the lava flows, small domes and pits are observed locally in the western side of Verdandi Corona. Lava flows are overlain by a set of narrow, 200 km long, bright, linear features, approximately oriented E–W, and also crosscutting Verdandi Corona. They correspond to faults. Verdandi Corona corresponds to a circular depression bounded by a series of discontinuous, concentric, linear features. The detailed analysis of these features shows that they are characterized by a pair of topographic scarps where the western one is outlined by a radar-bright response and the opposite one is characterized by a narrow, radar-dark response. The pairs of discontinuous, concentric scarps bounding a

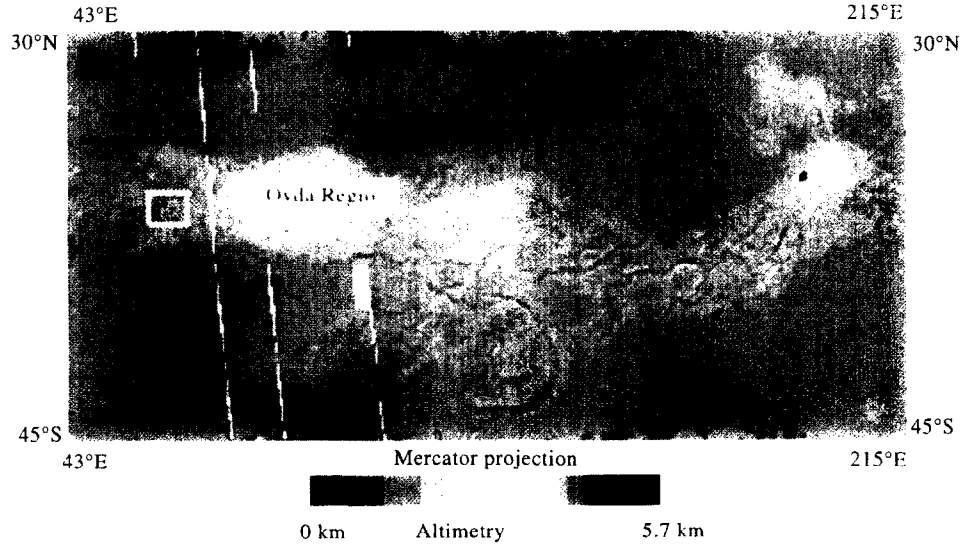

Fig. 1. Magellan altimetric map of Aphrodite Terra (NASA-JPL). It covers an area of 18,000 km (E–W) by 7875 km (N–S) in Mercator projection. Ovda Regio (bright area) is located on the western part of Aphrodite Terra and its altitude reaches 3 km. The white box indicates the extended image of Magellan radar F-MIDRP.05S065

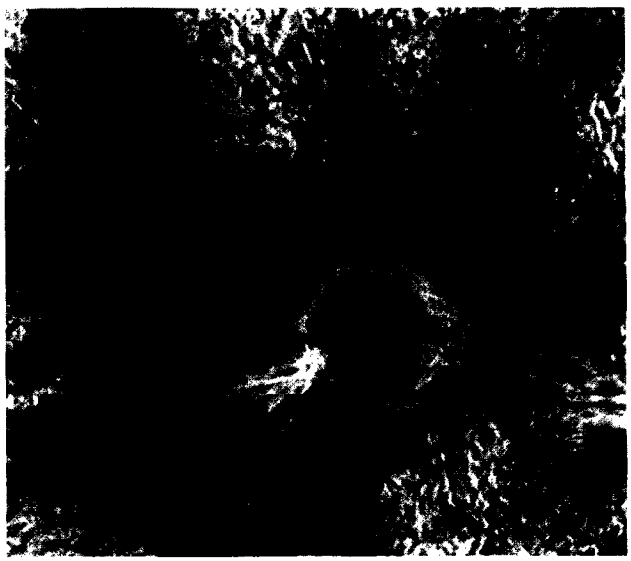

Fig. 2. Magellan full-resolution radar mosaic F-MIDRP.05S065, centred at latitude 05°S and longitude 65°E. It covers an area of approximately 500 km in latitude × 560 km in longitude. The radar illumination is oriented to the east, with a 44° incidence angle

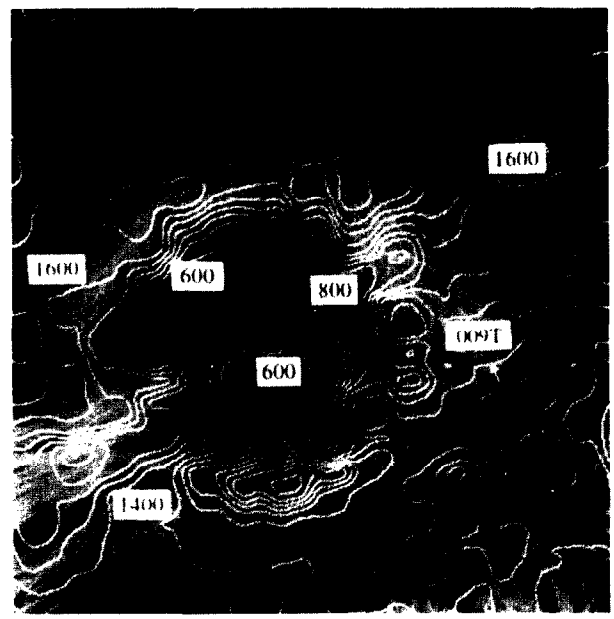

Fig. 3. Magellan altimetry superposed on Magellan radar image centred on Verdandi Corona (5°S–65°E). The image is approximately 200 km × 200 km. Spacing of contour lines is 200 m

Fig. 4. Structural interpretation of radar mosaic F-MIDRP.05S065. The hand-drawn map (A) presents most of the structures, and gives their tectonic styles (1, fault; 2, normal fault) (Ansan, 1993). The numerical processing (B) enhances the interpretation, and outputs the quantitative parameters of all structures (Blondel, 1992)

trough are interpreted as ring-shaped fractures or grabens. As indicated by altimetry (Fig. 3), blocks bounded by ring-shaped fractures or grabens tend to slump into the depression. Altogether, these geometric characteristics suggest that Verdandi Corona is similar to a volcanic caldera that would result from the collapse of an old volcano. The caldera would be probably associated with igneous features such as those of a ring complex (Price and Cosgrove, 1990).

From the crosscutting and/or superposition relationships of the structures previously mentioned, a relative chronology can be outlined. In a first stage, the pattern of radar-bright blocks formed the substratum. In an extensional tectonic regime, this substratum divided into a mosaic of horsts and grabens, oriented N–S, NNE–SSW and NW–SE. A second stage saw the filling of grabens with lava flows (radar-dark troughs), possibly originating from the observed circular Verdandi Corona, which may have been a volcano at this stage. In the third stage, this volcano collapsed because of magma withdrawal from below the caldera. In the fourth stage, Verdandi Corona was crosscut by a network of long, linear, faults oriented approximately E–W. Therefore, this region is interpreted as formed in extensional tectonic regime associated with volcanic activity (Ansan, 1993).

The same image with a reduced-resolution version of the F-MIDRP.05S065 (browse image) has been numerically processed (Fig. 4B; Blondel, 1992; Blondel *et al.*, 1992). The pixel size is then 600 m instead of 75 m. The Structure-Tracking algorithm computes for each detected structure its length, direction and sinuosity. A histogram of lengths displays three classes (Fig. 5A): 0–20 pixels (0–12 km), 20–50 pixels (12–30 km), and 50+ pixels (more than 30 km). For each class, a rose diagram of the cumulated lengths in each direction (Fig. 5B) shows a bimodal distribution of tectonic structures, with peaks at N120° ± 15° and N215° ± 5°. The rose diagram for longer features exhibits a marked peak at N105°. It corresponds to the linear faults overcutting Verdandi Corona (Fig. 2). On the same rose diagram, the peak close to N180° originates from detection of the radar gap boundaries. Peak directions, as established from these diagrams, corroborate and enhance those seen through the classic method of image interpretation. Other information, unobtainable by hand, can be gathered from the use of sinuosity. Sinuosity is the ratio of Euclidian distance between the tips of the feature and its actual length. The higher the sinuosity, the more sinuous the structure. Plotting the sinuosity of all medium (20–50 pixels) structures in respect to their directions again shows the existence of two main directions: N102° ± 15° and N125° ± 5° (Fig. 5C left). Low sinuosities are concentrated around N105°, whereas all directions exhibit higher sinuosities, i.e. structures in these directions are more sinuous. A map of features with sinuosity between 1 and 1.1 shows that they mainly represent the quasi-linear faults crosscutting Verdandi Corona. Numerical processing allows the structural interpretation to be improved by quantifying the geometric parameters of linear features.

Discussion and conclusion

A model of the chronologic evolution of this area is proposed based on classic image interpretation and digital processing (Fig. 6). During the first stage, the blocks constituting the basement undergo crustal stretching (Fig. 6.1). A mosaic of horsts and grabens results thereof, the grabens having a near constant length of about 30 km. Two main trends of fracturation are detected: N120° ± 15° and N215° ± 5°, quasi-orthogonal. During the second stage (Fig. 6.2), volcanic activity leads to the embayment of the grabens with a dark material corresponding to fluid lava flows. This volcanic material could relate either to flows similar to basaltic traps, or to the great circular feature, Verdandi Corona, interpreted as a volcano. In a later stage (Fig. 6.3), the volcano collapse produces the network of concentric and radial fractures. In the last stage (Fig. 6.4), the old collapsed volcano is

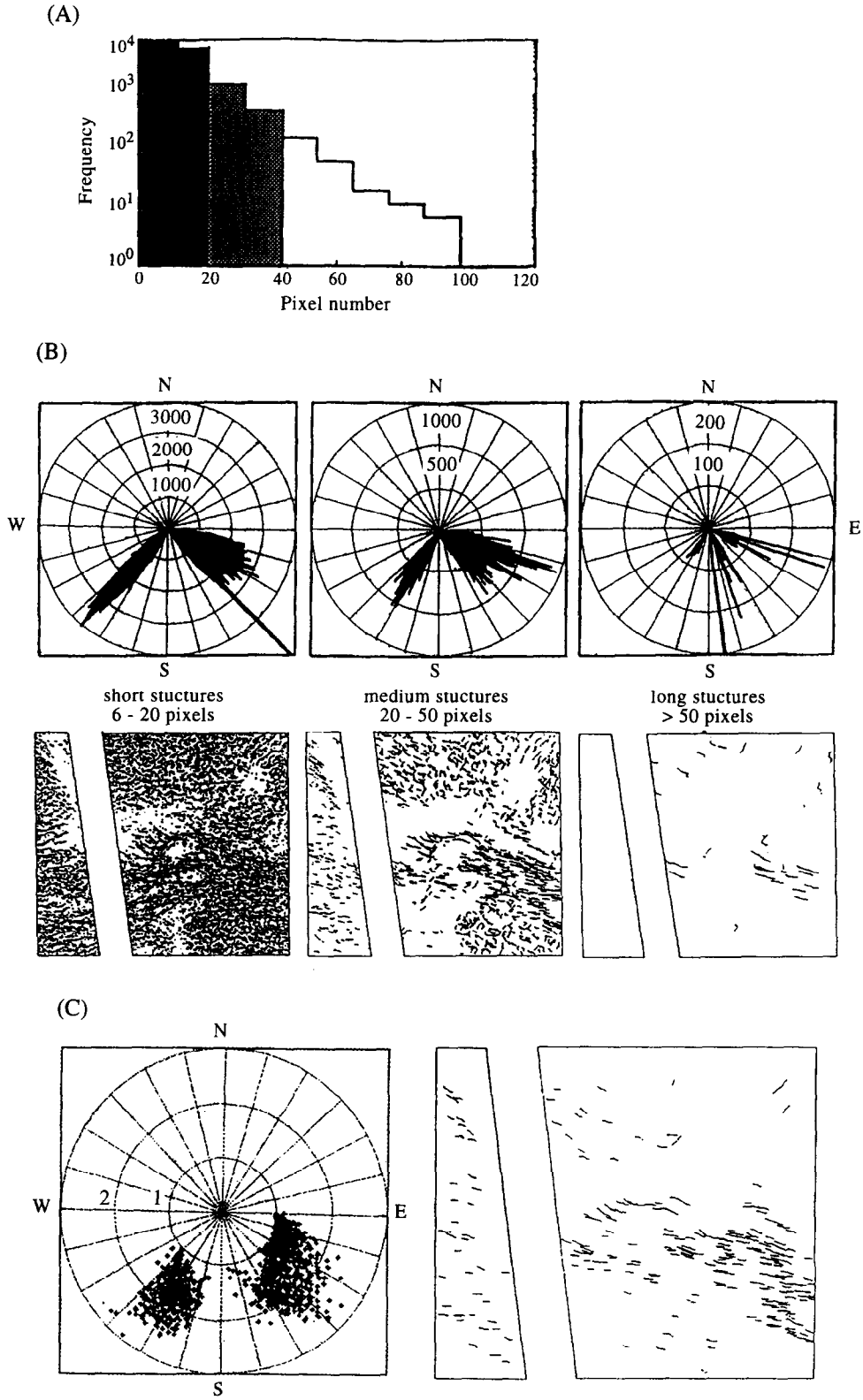

Fig. 5. (A) Histogram for the number of pixels of all structures numerically detected. Three classes of structures: short (0–20 pixels/10–12 km), medium (20–50 pixels/112–30 km), and long (50+ pixels/30+ km). (B) Rose diagrams for short, medium and long structures with corresponding maps. (C) Polar plot analogous to rose diagram for sinuosity of medium structures and map of the sublinear ones

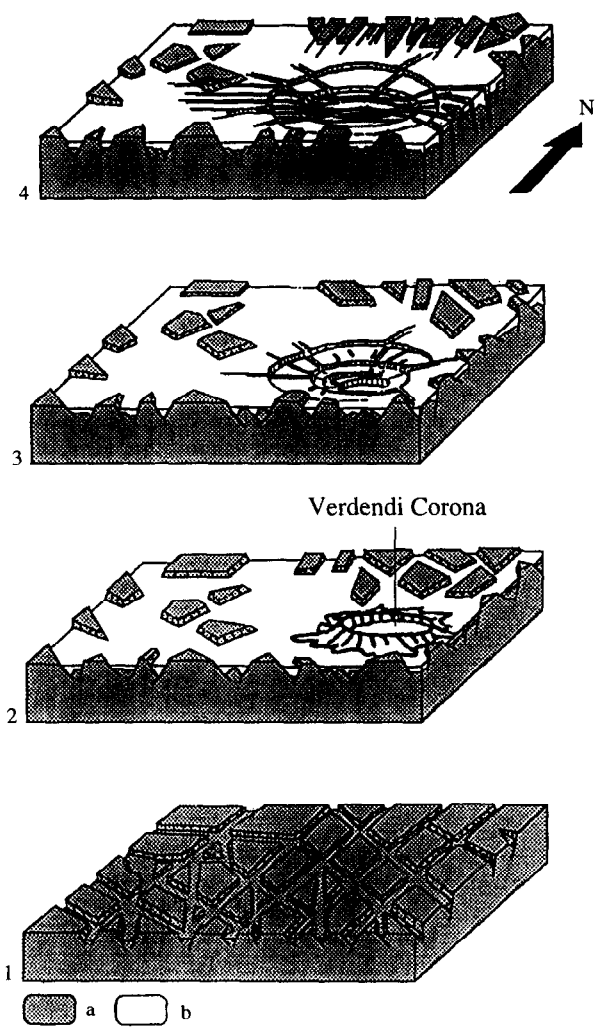

Fig. 6. Proposed model for the chronological evolution of the westernmost part of Aphrodite Terra. Stage 1: fracturation. Stage 2: volcanic flooding and magmatic intrusion. Stage 3: collapse of the old volcano called Verdandi Corona. Stage 4: N105° faults overcut Verdandi Corona. (a) Substratum; (b) lava flows

crosscut by a network of long rectilinear faults oriented N105°.

The studied area belongs to Ovda Regio, the westernmost part of Aphrodite Terra, characterized by highly deformed terrains often defined by a complex ridged terrain unit (Solomon *et al.*, 1992; Bindschadler *et al.*, 1992). They have interpreted the radar-bright blocks as ridges resulting from compressive deformation. Then, these ridges are crosscut by later fracturing, which implies that the crustal shortening was followed by modest extension.

Based on radar altimetry, imagery and gravimetry, several theories have been proposed to explain the formation and evolution of western Aphrodite Terra. For some, the complex ridged terrain of Ovda Regio would be the manifestation at the surface either of the lithospheric extension or mantle upwelling (Crumpler *et al.*, 1987; Morgan and Phillips, 1983; Griffiths and Campbell, 1991; Herrick and Phillips, 1990; Stofan and Saunders, 1990; Phillips *et al.*, 1991; Kiefer and Hager, 1991; Bindschadler *et al.*, 1992). Conversely, Bindschadler and Parmentier (1990) and Bindschadler *et al.* (1992) propose that the complexed ridged terrain would result from mantle downwelling ("coldspot"). Our detailed structural study of high-resolution Magellan radar image favours the model of formation in a mantle upwelling context. The regional crustal deformation, whose results have been observed and quantified, would originate from the ascending and flattening of a diapir intruded in the Venusian crust. The ascending diapir would have led to a topographic uplift (2 km in elevation). And, in response to this domal uplift, radiating fracturation would have developed in a 2000 km wide circular zone. The observed pattern of horsts and grabens could be associated with dike emplacement above a shallow magma reservoir. The ascending diapir would be associated with the volcanic activity which led to embayment of all the grabens and intrusion of basalt, forming a thick crust. The high regional correlation between topography and geoid anomaly (35 m) and gravity anomaly (35 mgal), and the high compensation depth (70 km) computed both with PVO data and Magellan data (Ananda *et al.*, 1980; Sjogren *et al.*, 1983; Herrick *et al.*, 1989; Black *et al.*, 1991; Smrekar and Phillips, 1991) seem to indicate that Ovda Regio formed above a mantle upwelling or mantle diapir.

As we saw previously, at the centre of Ovda Regio, there is a corona called Verdandi. This structure is defined by Stofan *et al.* (1992) as a concentric, and well-defined tectonic annulus that displays a moderate number of associated features. The observed tectonic structures (concentric grabens associated with radial fractures) and volcanic flows are similar to the structures forming above an ascending diapir as shown in analogic experiments and numeric models (Griffiths and Campbell, 1991; Herrick and Phillips, 1990; Stofan *et al.*, 1992; Squyres *et al.*, 1992). From these models, the corona formation can be summed up in three stages and applied to Verdandi Corona. First, a 100 km in diameter diapir rises through the Venusian lithosphere leading to a dome formation. The ascending strengths of the diapir being sufficiently high, the crust breaks up in a radial manner above the diapir. Second, the diapir spreads and flattens. During this stage, volcanism and magmatic intrusion occur and a volcano rises above the surface (Verdandi). Third, because of the emptying of the magmatic reservoir and the withdrawal of the dynamic support of the diapir, the volcano collapses, marked by concentric fracturations and forming Verdandi Corona.

Throughout this study, we have detailed the structural geology of Verdandi Corona and the surrounding region. The interpretations were quantified by combining conventional mapping and image processing techniques, enabling the establishment of a relative chronology. The resulting model of formation and evolution of Verdandi Corona supports and is supported by the larger-scale interpretation of Ovda Regio (Herrick *et al.*, 1989; Stofan *et al.*, 1992; Squyres *et al.*, 1992). The mechanisms of formation of fractured terrains in Ovda Regio and Verdandi Corona are similar (diapirs) but at different scales. The 1000 km scale for Ovda Regio would imply a process associated to mantle convection at a lithospheric scale,

whereas the 100 km scale of Verdandi Corona argues for a crustal-scale process. The small diapir at the origin of Verdandi Corona could very well be a local upwelling of magma from the regional Ovda diapir through a local pre-existing crustal weakness.

Acknowledgements. Most of this work was accomplished when both authors were in Orsay. Funding from ATP Planétologie (contract No. 893710-02) of INSU is gratefully acknowledged. The Magellan data used in this study were made available through the Photothèque Planétaire d'Orsay, NASA Regional Planetary Image Center. The authors thank Pierre Vergely, Christophe Sotin and Philippe Masson for their constructive comments and discussion throughout this study.

References

Ananda, M. P., Sjogren, W. L., Phillips, R. J., Winberly, R. N. and Bills, B. G., A low order global gravity field of Venus and dynamical implications. *J. Geophys. Res.* **85,** 8295–8302, 1980.

Ansan, V., Interprétations géologiques et structurales de Vénus à partir des images radar Venera 15–16 et Magellan (Geologic and structural interpretations of Venus based on Venera 15–16 and Magellan radar images). Ph.D. Thesis, Univ. Paris-Sud, Orsay, France, 270 pp., 1993.

Bindschadler, D. L. and Parmentier, E. M., Mantle flow tectonics: the influence of a ductile lower crust and implications for the formation of topographic uplands on Venus. *J. Geophys. Res.* **95,** 21329–21344, 1990.

Bindschadler, D. L., Schubert, G. and Kaula, W. M., Cold spots and hot spots: global tectonics and mantle dynamics of Venus. *J. Geophys. Res.* **97,** 13495–13532, 1992.

Black, M. T., Zuber, M. T. and McDoo, D. C., Comparison of observed and predicted gravity profiles over Aphrodite Terra, Venus. *J. Geophys. Res.* **96,** 301–315, 1991.

Blondel, Ph., Traitement et interprétation des données radar: applications à l'étude de la surface de Vénus (Processing and interpretation of radar data: applications to the study of the surface of Venus). Ph.D. Thesis, Univ. Paris-VII, Jussieu, France, 327 pp., 1992.

Blondel, Ph., Sotin, C. and Masson, Ph., Automatic determination of line structures for processing the Magellan data: tests on Venera 15/16 images. *EOS Trans. A.G.U.* **71,** 1990.

Blondel, Ph., Sotin, C. and Masson, Ph., Adaptive filtering and struture-tracking for statistical analysis of linear features: applications to radar images of Venus. *Comput. Geosci.* **18,** 1169–1184, 1992.

Blondel, Ph., Sempéré, J.-C. and Robigou, V., Textural analysis and structure-tracking for geological mapping: applications to sonar data from Endeavour segment, Juan de Fuca Ridge, *Proc. OCEANS'93, IEEE-OES*, pp. 209–213. Victoria, B.C., 1993.

Crumpler, L. S., Head, J. W. and Harmon, J. K., Regional linear cross-strike discontinuities in Western Aphrodite Terra. *Geophys. Res. Lett.* **14,** 607–610, 1987.

Ford, J. P., Blom, R. G., Crisp, J. A., Elachi, C., Farr, T. G., Saunders, R. S., Theilig, E. E., Wall, S. D. and Yewell, S. B., Spaceborne radar observations: a guide for Magellan radar image analysis. JPL Publication 89-41, 125 pp., 1989.

Ford, J. P., Plaut, J. J., Weitz, C. M., Farr, T. G., Senske, D. A., Stofan, E. R., Michaels, G. and Parken, T. J., Guide to Magellan image interpretation. JPL Publication 93-24, 148 pp., 1993.

Griffiths, J. H. and Campbell, R. W., Interaction of mantle plume heads with the Earth surface and on-set of small-scale convection. *J. Geophys. Res.* **96,** 18295–18310, 1991.

Hagfors, T., Backscattering from an undulating surface with applications to radar returns from the Moon. *J. Geophys. Res.* **69,** 3779–3784, 1964.

Herrick, R. R. and Phillips, R. J., Blob tectonics: a prediction for Western Aphrodite Terra, Venus. *Geophys. Res. Lett.* **17,** 2129–2132, 1990.

Herrick, R. R., Bills, B. G. and Hall, S. A., Variations in effective compensation depth across Aphrodite Terra, Venus. *Geophys. Res. Lett.* **16,** 543–546, 1989.

Kiefer, W. S. and Hager, B. H., A mantle plume model for the equatorial highlands of Venus. *J. Geophys. Res.* **91,** 403–419, 1991.

Leberl, F. W., Thomas, J. K. and Maurice, K. E., Initial results from the Magellan stereo experiment. *J. Geophys. Res.* **97,** 13675–13689, 1992.

Luxey, P., Parson, L. M. and Murton, B. J., Magmatic and tectonic interaction in the iceland region. *Proc. Remote Sensing Soc.*, pp. 503–511, 1995.

McKenzie, D., McKenzie, J. M. and Saunders, R. S., Dike emplacement on Venus and on Earth. *J. Geophys. Res.* **97,** 15977–15990, 1992.

Morgan, P. and Phillips, J. J., Hot-spot heat transfer: its application to Venus and implications to Venus and Earth. *J. Geophys. Res.* **88,** 8305–8317, 1983.

Phillips, R. J. and Malin, M. C., *The Interior of Venus and Tectonic Implications in Venus* (edited by D. Hunten, L. Colin and V. I. Moroz), pp. 159–214. Univ. of Arizona Press, Tucson, 1983.

Phillips, R. J., Grimm, R. E. and Malin, M. C., Hot-spot evolution and the global tectonics of Venus. *Science* **252,** 651–658, 1991.

Price, N. J. and Cosgrove, J. W., Diapirs related structures and circular features, in *Analysis of Geological Structures*, pp. 89–122. Cambridge Univ. Press, London, 1990.

Saunders, R. S. and Pettengill, G. H., Magellan: mission summary. *Science* **252,** 247–252, 1991.

Saunders, R. S., Arvidson, R. E., Head, J. W., Schaber, G. G., Stofan, E. R. and Solomon, S. C., An overview of Venus geology. *Science* **252,** 249–252, 1991.

Saunders, R. S., Spear, A. J., Allin, P. C., Austin, R. S., Berman, A. L., Chandlee, R. C., Clark, J., de Charon, A. V., Jong, E. M., Gunn, D. J., Hensley, S., Johnson, W. T. K., Kirby, C. E., Leung, K. S., Lyons, D. T., Michaels, G. A., Miller, J., Morris, R. B., Morrison, A. D., Piereson, R. G., Scott, J. F., Shaffer, S. J., Slonski, J. P., Stofan, E. R., Thompson, T. W. and Wall, S. D., Magellan mission summary. *J. Geophys. Res.* **97,** 13067–13090, 1992.

Schaber, G. G., Berlin, G. L. and Brown, W. E., Variations in surface roughness within Death Valley, California: geologic evaluation of 25-cm-wavelength radar images. *Geol. Soc. Am. Bull.* **87,** 29–41, 1976.

Sjogren, W. L., Bills, B. G., Bireland, P. W., Esposito, P. B., Konopliv, A. R., Mottinger, N. A., Ritke, S. J. and Phillips, R. J., Venus gravity anomalies and their correlation with topography. *J. Geophys. Res.* **88,** 1119–1128, 1983.

Smrekar, S. and Phillips, R. J., Venusian highlands: geoid to topography ratios and their implications. *Earth Planet. Sci. Lett.* **107,** 582–597, 1991.

Solomon, S. C. and Head, J. W., Fundamental issues in geology and geophysics of Venus. *Science* **252,** 252–260, 1991.

Solomon, S. C., Smrekar, S. E., Bindschadler, D. L., Grimm, R. E., Kaula, W. M., McGill, G. E., Phillips, R. J., Saunders, R. S., Schubert, G., Squyres, S. W. and Stofan, E. R., Venus tectonics: an overview of Magellan observations. *J. Geophys. Res.* **97,** 13199–13257, 1992.

Squyres, S. W., Janes, D. M., Baer, G., Bindschadler, D. L., Schubert, G., Sharpton, V. L. and Stofan, E. R., The morphology and evolution of coronae on Venus. *J. Geophys. Res.* **97,** 13611–13635, 1992.

Stofan, E. R. and Saunders, R. S., Geologic evidence of hotspot activity on Venus: predictions for Magellan. *Geophys. Res. Lett.* **17,** 1377–1380, 1990.

Stofan, R. E., Sharpton, V. L., Schubert, G., Baer, G., Bindschadler, D. L., Janes, D. M. and Squyres, S. W., Global distribution and characteristics of coronae related features on Venus: implications for origin and relation to mantle processes. *J. Geophys. Res.* **97,** 13347–13378, 1992.

Ulaby, F. T., Moore, R. K. and Fung, A. K., Microwave remote sensing: active and passive, in *Radar Remote Sensing and Surface Scattering and Emission Theory*, Vol. 2. Addison-Wesley, Reading, Massachusetts, 1982.